Model-based Prognostic Techniques

Jianhui Luo, Madhavi Namburu, Krishna Pattipati
Dept. of ECE, University of Connecticut
Storrs, CT-06269, USA
Email: krishna@engr.uconn.edu

Liu Qiao, Masayuki Kawamoto, Shunsuke Chigusa
Toyota Technical Center U.S.A.
1555 Woodridge, RR#7
Ann Arbor, MI 48105, USA

Abstract— Conventional maintenance strategies, such as corrective and preventive maintenance, are not adequate to fulfill the needs of expensive and high availability industrial systems. A new strategy based on forecasting of system degradation through a prognostic process is required. The recent advances in model-based design technology have realized significant time savings in product development cycle. These advances facilitate the integration of model-based diagnosis and prognosis of systems, leading to condition-based maintenance and increased availability of systems. With an accurate simulation model of a system, diagnostics and prognostics can be synthesized concurrently with system design.

In this paper, we will develop an integrated prognostic process based on data collected from model-based simulations under nominal and degraded conditions. Prognostic models are constructed based on different random load conditions (modes). Interacting Multiple Model (IMM) is used to track the hidden damage. Remaining life prediction is performed by mixing mode-based life predictions via time-averaged mode probabilities. The solution has the potential to be applicable to a variety of systems, ranging from automobiles to aerospace systems.

I. Introduction

Conventional maintenance strategies consist of corrective and preventive maintenance. In corrective maintenance, the system is maintained on an "as-needed" basis, usually after a major breakdown [1]. In preventive maintenance, components are replaced based on a conservative schedule to "prevent" commonly occurring failures. Although preventive maintenance programs increase system availability, they are expensive because of frequent replacement of costly parts before the end of their life. Another disadvantage of preventive maintenance is that it is time-based. Studies have revealed that most of the equipment failures are not related to the number of hours they were operated. Hence, time-based solutions are not cost-effective. Consequently, these conventional maintenance strategies are not adequate to fulfill the needs of expensive and high availability industrial systems. Condition-based predictive maintenance is an alternative that uses embedded diagnostics and prognostics to determine system's health. Failure prognosis involves forecasting of system degradation based on observed system condition.

The recent advances in model-based design technology have resulted in significant time savings in product development cycle. A number of applications of model-based design can be found in automotive, aerospace and defense industries. Because system model is simulated early in the design stage, the reliability and robustness of the system are ultimately increased. These advances facilitate the integration of model-based diagnosis and prognosis of systems, leading to condition-based maintenance and increased availability of systems. With an accurate simulation model of a system, diagnostics and prognostics can be synthesized concurrently with system design.

In our previous paper [2], we have developed an intelligent model-based diagnostic procedure that combines quantitative and graph-based dependency models. The hybrid model-based diagnostic method not only improves the diagnostic system's accuracy and consistency of those based solely on a graph-based model, but also exploits the existing validated knowledge on rule-based methods, enables rapid remote diagnosis, and responds to the challenge of increased system complexity. The hybrid model-based diagnostic process was demonstrated on an anti-lock braking system. In this paper, the focus of our application is on prognosis (remaining life prediction) of an automotive suspension system. However, the solution is generic and has the potential for application in a wide range of systems.

The paper is organized as follows. Section 2 presents an overview of the proposed intelligent model-based diagnostic/prognostic design process [2]. Section 3 reviews the current prognostic techniques. Section 4 illustrates the prognostic model formulation and remaining life estimation algorithms. Section 5 reports on a demonstration of the prognostic procedure on a suspension system. Section 6 concludes the paper with a summary and future research directions.

II. Intelligent Model-based Diagnosis/Prognosis

A systems-oriented approach to prognostics requires that the failure detection and inspection-based methods be augmented with forecasting of parts degradation, mission criticality and decision support. Such prognostics must deal not only with the condition of individual components, but also the impact of this condition on the mission-readiness and the ability to take appropriate actions. However, such a continuous health management system must be carefully engineered at every stage of a system design, operation and maintenance.

Fig. 1 shows the block diagram of the proposed intelligent diagnostic and prognostic process. The process seamlessly employs graph-based dependency models for fault diagnosis, and quantitative (analytical) models for test design and fault detection. It contains six major blocks: model, sense, develop

0-7803-7837-7/03/$17.00 ' 2003 IEEE

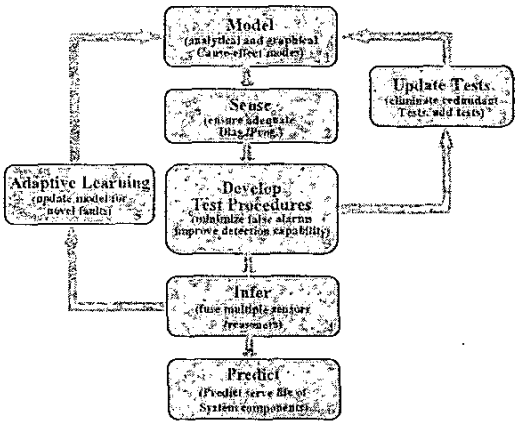

Fig. 1. Intelligent diagnostic/prognostic process

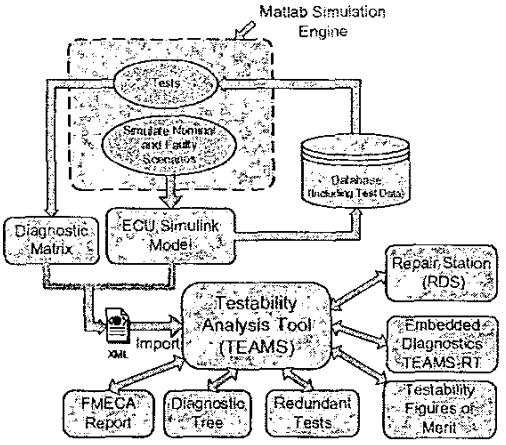

Fig. 2. Hybrid modeling approach

and update test procedures, infer, adaptive learning and predict.

Step 1: Model

In this step, models to understand fault-to-error characteristics of system components are developed. This is achieved by a hybrid modeling technique, which combines quantitative models (simulation models) and graphical cause-effect models in the failure space, through an understanding of the failure modes and their effects, physical/behavioral models, and statistical and learning techniques based on actual failure progression data (e.g., field failure data) as applied to system components. Fig. 2 illustrates the block diagram of the hybrid modeling approach for an automotive system controlled by an electrical control unit (ECU). The quantitative model is assumed to be a representative sample available in the MATLAB/SIMULINK® design environment. These require extensive simulations (for nominal and faulty scenarios) to extract the relationships between failure causes and observable effects of the system. Information on the system model, such as model parameters, test definitions and simulation data, is stored in a database.

The cause-effect model, in the form of a Diagnostic Matrix (D-Matrix), is extracted through fault simulations on the quantitative model using tests defined in the model. After the D-matrix is generated, this matrix and other available system information (such as the location of faults) from the MATLAB/SIMULINK® environment are exported in an Extensible Markup Language (XML) format. XML is a flexible text format and is increasingly playing a significant role in the exchange of a wide variety of data on the Web and among many different modeling environments. The XML file is imported into a diagnostic analysis tool, such as TEAMS® (Testability Engineering And Maintenance System) [3], to automatically layer in the cause-effect dependencies on a structural model. TEAMS® computes percent fault detection and isolation measures, identifies redundant tests and ambiguity groups, and generates updated Failure Modes Effects and Criticality Analysis (FMECA) report and the diagnostic tree. It also exports the D-matrix, the test code and structural information to TEAMS-RT® for on-board, real-time diagnosis. The onboard diagnostic data is seamlessly downloaded to TEAMS-RDS® (remote diagnosis server) for interactive diagnosis (by driving interactive electronic technical manuals), diagnostic/maintenance data management, logging and trending. The TEAM-RDS® can also be integrated with the supply-chain systems and logistics databases for company-wide vehicle health management.

Step 2: Sense

The sensor suite is typically designed for vehicle control and performance. The efficacies of these sensors are systematically evaluated and quantified to ensure that adequate diagnosis and prognosis are achievable. If the existing sensor suite is not appropriate for diagnosis/prognosis, use of additional sensors and/or analytical redundancy must be considered without impacting vehicle control and performance. Diagnostic analysis by TEAMS® can be used to compare and evaluate alternative sensor placement schemes.

Step 3: Develop and Update Procedures

Smart test procedures that detect failures, or onset thereof, have to be developed. These procedures have to be carefully tuned to minimize false alarms, while improving their detection capability (power of the test). The procedures should have the capability to detect trends and degradation and assess the severity of a failure for early warning.

Step 4: Infer

An integrated on-board and off-board reasoning system capable of fusing results from multiple sensors/reasoners and driver (or "driver model") to evaluate the health of the vehicle needs to be applied. This reasoning engine and the test procedures should be compact enough so that they can be embedded in the ECU and/or a diagnostic maintenance computer. In the proposed approach, the test code and TEAMS-RT® are embedded in a real-time operating system to process the sensor data and to provide inference results. If on-board diagnostic data is downloaded to a repair station, TEAMS-RDS® is used

to provide assistance to repair personnel in rapidly identifying replaceable component(s).

Step 5: Adaptive Learning

If the observed fault signature does not correspond to faults modeled in the graphical dependency model, system identification techniques are invoked to identify new cause-effect relationships, to update the D-matrix and to layer in this information onto TEAMS® model.

Step 6: Predict

Lifing algorithms, which interface with onboard usage monitoring systems and parts management databases, are used to predict the useful life remaining of system components.

In [2], we have demonstrated Steps 1, 2, 3 and 4. In the rest of the paper, we focus on Step 6 and demonstrate it on an automotive suspension system.

III. Prognostic Techniques

Many industrial systems exhibit increasing wear and tear of equipment during operation [4]. For example, an automobile has many pieces of equipment, such as the engine, gear box and valves that exhibit various types of performance degradation due to erosion, friction, internal damage and cracks. Prognostics are viewed as an add on capabilities to diagnosis; they assess the current health of a system and predict its remaining life based on features that capture the gradual degradation in the operational capabilities of a system. Prognostics are critical to improve safety, plan successful missions, schedule maintenance, reduce maintenance cost and down time [5]. Unlike fault diagnosis, prognosis is a relatively new area and became an important part of Condition-based Maintenance (CBM) of systems. Currently, there are many prognostic techniques; their usage must be tuned for each application. The prognostic methods can be classified as being associated with one or more of the following two approaches: **data-driven** and **model-based** [6]. Each of these approaches has its own advantages and disadvantages, and, consequently they are often used in combination in many applications. This section will provide an overview of the prognostic techniques and their applications.

A. Data-driven Prognostics

The data-driven approaches are derived directly from routinely monitored system operating data (e.g., calibration, calorimetric data, spectrometric data, power, vibration and acoustic signal, temperature, pressure, oil debris, currents, voltages). In many applications, measured input/output data is the major source for gaining a deeper understanding of the system degradation behavior. The data-driven approaches rely on the assumption that the statistical characteristics of data are relatively unchanged unless a malfunctioning event occurs in the system. That is, the *common cause variations* are entirely due to uncertainties and random noise, where as *special cause variations* (e.g., due to degradations) account for data variations not attributed to common causes.

The data-driven approaches are based on statistical and learning techniques from the theory of pattern recognition. These range from multivariate statistical methods (e.g., static and dynamic principle components (PCA), linear and quadratic discriminants, partial least squares (PLS) and canonical variate analysis (CVA)), to black-box methods based on neural networks (e.g., probabilistic neural networks (PNN), decision trees, multi-layer perceptrons, radial basis functions and learning vector quantization (LVQ)), graphical models (Bayesian networks, hidden Markov models), self-organizing feature maps, signal analysis (filters, auto-regressive models, FFT, etc.) and fuzzy rule-based systems.

The research on data-driven approaches has focused on monitoring of signals related to system health. In [7], a prognostic process for transmission gears is proposed by modeling the vibration signal as a Gaussian mixture. By adaptively identifying and tracking the changes in the parameters of Gaussian mixture, it is possible to predict gear faults. Wang [8] used an AR process to model a vibration signal for prognosis. However, the AR parameters (polynomial coefficients) have no physical meaning related to the monitored system. Zhang [9] proposed a parameter estimation approach for a nonlinear model with temperature measurements of gas turbines. The on-line detection procedure presented in [9] can track small variations in parameters for early warning. In [10], a dynamic wavelet neural network (DWNN) was implemented to transform sensor data to the time evolution of a fault pattern and predict the remaining useful time of a bearing. The DWNN model was first trained by using vibration signals of defective bearings with varying depth and width of cracks, and then was used to predict the crack evolution until the final failure. Swanson [11] proposed to use a Kalman filter to track the dynamics of the mode frequency of vibration signals in tensioned steel band (with seeded crack growth). In [12], Garga proposed a signal analysis approach for prognostics of an industrial gearbox. The main features used included the root mean square (RMS) value, Kurtosis and Wavelet magnitude of vibration data.

The strength of data-driven techniques is their ability to transform high-dimensional *noisy* data into lower dimensional information for diagnostic/prognostic decisions. The main drawback of data-driven approaches is that their efficacy is highly-dependent on the quantity and quality of system operational data. The data-driven approach is applicable to systems, where an understanding of first principles of system operation is not comprehensive.

B. Model-based Prognostics

The model-based methods assume that an accurate mathematical model is available. The model-based methods use residuals as features, where the residuals are the outcomes of consistency checks between the sensed measurements of a real system and the outputs of a mathematical model. The premise is that the residuals are large in the presence of malfunctions, and small in the presence of normal disturbances, noise and modeling errors. Statistical techniques are used to define thresholds to detect the presence of faults. The three main ways of generating the residuals are based on parameter esti-

mation, observers (e.g., Kalman filters, reduced order unknown input observers, Interacting Multiple Models [13]) and parity relations. The model-based approach is applicable in situations where accurate mathematical models can be constructed from first principles.

Adams [14] proposed to model damage accumulation in a structural dynamic system as first/second order nonlinear differential equations. Chelidze [15] modeled degradation as a "slow-time" process, which is coupled with a "fast-time", observable subsystem. The model was used to track battery degradation (voltage) of a vibrating beam system.

The main advantage of model-based approach is the ability to incorporate physical understanding of the system to monitoring. Another advantage is that, in many situations, the changes in feature vector are closely related to model parameters [16]. Therefore, it can also establish a functional mapping between the drifting parameters and the selected prognostic features. Moreover, if understanding of the system degradation improves, the model can be adapted to increase its accuracy and to address subtle performance problems. Consequently, it can significantly outperform data-driven approaches.

In the next section, we will focus on model-based prognostic techniques by combining singular perturbation methods of control theory, coupled with dynamic state estimation techniques for damage prediction.

IV. Model-based Prognostic Techniques

Fig. 3 shows the block diagram of our model-based prognostic process. This process consists of six steps for predicting the remaining life of a system.

A. Identify system model (Step 1)

We consider the degradation model of a system of the following form:

$$\begin{aligned} \dot{\mathbf{x}} &= \mathbf{f}(\mathbf{x}, \boldsymbol{\lambda}(\boldsymbol{\theta}), \mathbf{u}) \\ \dot{\boldsymbol{\theta}} &= \epsilon \mathbf{g}(\mathbf{x}, \boldsymbol{\theta}) \\ \mathbf{y} &= \mathbf{C}\mathbf{x} + \mathbf{D}\mathbf{u} + \mathbf{v} \end{aligned} \tag{1}$$

where $\mathbf{x} \in \mathbf{R}^n$ is the set of state variables associated with the fast dynamic behavior of the system; $\boldsymbol{\theta} \in \mathbf{R}^m$ is the set of slow dynamic variables related to system damage (degradation); $\mathbf{u} \in \mathbf{R}^l$ is the input vector; the parameter vector $\boldsymbol{\lambda} \in \mathbf{R}^q$ is a function of $\boldsymbol{\theta}$; the rate constant $0 < \epsilon \ll 1$ defines the time-scale separation between the fast dynamics and the slow drift [15]; $\mathbf{y} \in \mathbf{R}^p$ is the output vector and $\mathbf{v}$ is the measurement noise. Since ϵ is very small, Eq. (1) can be considered as a system with slowly drifting parameters.

This approach is closely related to a standard singular perturbation model proposed by Kokotović [17]. The only difference is that, in the "fast-time" process, $\boldsymbol{\lambda}(\boldsymbol{\theta})$ is replaced by just $\boldsymbol{\theta}$. In the limit as $\epsilon \to 0$, we obtain the so-called *associated system* [18]:

$$\begin{aligned} \dot{\mathbf{x}} &= \mathbf{f}(\mathbf{x}, \boldsymbol{\lambda}(\boldsymbol{\theta}_0), \mathbf{u}) \\ \dot{\boldsymbol{\theta}} &= 0 \end{aligned} \tag{2}$$

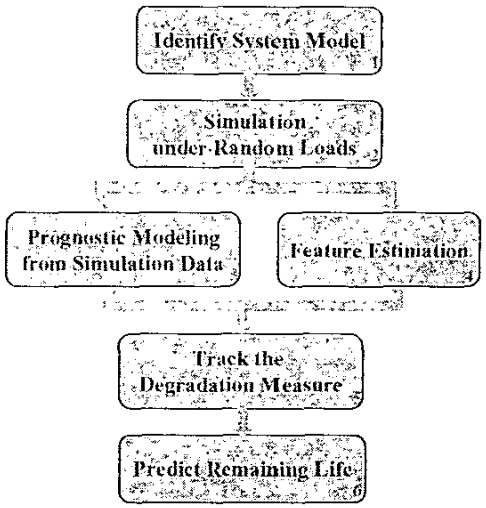

Fig. 3. Model-based prognostic process

The *slow manifold* [17] $\mathbf{x} = \mathbf{x}^*(\boldsymbol{\lambda})$, which is the solution to $\mathbf{f} = 0$ in Eq. (2), consists of equilibrium points. Thus, Eq. (1) can be viewed as a perturbation of Eq. (2) with slowly drifting parameters $\boldsymbol{\lambda}$.

In general, a first principles model of the hidden (damage) variable is not easy to obtain; the functional mapping between the damage variable and the system parameters is typically obtained from experimental data. For ease of exposition, in this paper, we consider the system of Eq. (1) with scalar quantities defined as $\mathbf{g} \equiv g$, $\boldsymbol{\lambda} \equiv \lambda$, $\epsilon \equiv \epsilon$ and $\boldsymbol{\theta} \equiv \theta$. This is a valid assumption if the scalar damage θ is independent of other damage variables, and is viewed as the most critical one in the system.

From a stochastic fatigue point of view [19], the damage variable θ is often related to crack growth and its value is equal to crack size. A widely used crack growth model is the Paris-Erdogan [20] law:

$$d\theta/dn = C(\Delta K)^{\gamma} \tag{3}$$

where $\Delta K = Y(\theta)(\Delta s)\sqrt{\pi\theta}$ is the stress intensity factor. $Y(\theta)$ accounts for the geometry of crack of the specimen, Δs is the stress range, C and γ are material constants. Typically C is a small number ($0 < C \ll 1$) and γ is in the range of 2 to 4. We can easily see that Eq. (3) can be written in the following general form:

$$d\theta/dn = \epsilon\phi_1(\theta)\phi_2(p) \tag{4}$$

where $\epsilon = C$, $\phi_1(\theta) = (Y(\theta)\sqrt{\pi\theta})^{\gamma}$, $p = \Delta s$ and $\phi_2(p) = p^{\gamma}$. The initial damage in above equation is $\theta(0) = \theta_0$.

The damage development law in Eq. (4) is a special case of that modeled in Eq. (1) if the parameter p can be represented as a function of $\mathbf{x}$, that is $p = h(\mathbf{x})$. Thus, $g(\mathbf{x}, \theta) = \phi_1(\theta)\phi_2(h(\mathbf{x}))$ in Eq. (1). Indeed, the damage evolution rules presented in [14], [15] follow Paris-Erdogan law modeled in

Eq. (4). The system model in Eq. (1) is more general in that the degradation law need not follow the Paris-Erdogan rule.

The value of damage variable θ can be arbitrary. To facilitate analysis, it is convenient to use a damage measure (or damage rate) ξ which takes values in the unit interval $[0, 1]$[1]. To transfer the slow-time process modeled in Eq. (1) to a process related to ξ, we will use the empirical Palmgren-Miner rule, which is used to estimate the life times of components subjected to a spectrum of loading. The Palmgren-Miner rule asserts that the damage fraction Δ_i at any stress level S_i is the ratio of n_i, the number of cycles of operation under this stress amplitude, to N_i, the total number of cycles that would produce a failure at that stress level. The total accumulated damage is then given by

$$\xi = \sum_{i=1}^{K} \Delta_j = \sum_{i=1}^{K} \frac{n_i}{N_i} \tag{5}$$

where K is the total number of stress levels. It is assumed that failure occurs if $\xi \geq 1$. Todinov [19] has proved that the Palmgren-Miner rule is compatible with the damage development law, if and only if the damage development rate $d\xi/dn$ at a constant parameter p (stress or strain amplitude) can be factored as a product of functions $\phi_1(\xi)$ and $\phi_2(p)$:

$$d\xi/dn = \eta\phi_1(\xi)\phi_2(p) \quad (0 < \eta \ll 1;\ \xi \in [0,\ 1]) \tag{6}$$

where $\eta\phi_1(\xi)\phi_2(p)$ is a non-negative function and n is the number of cycles. The load parameter p (usually the stress/strain amplitude) varies with cycles (time) [19].

To establish the relationship between Eq. (6) and the slow process in Eq. (1) for scalar damage variable, assume that Eq. (4) holds for M cycles with different loading amplitudes $\{p_i\}_{i=1}^{M}$. Under the i^{th} amplitude, the damage increases from $\theta_{i-1} \rightarrow \theta_i (i = 1, \ldots M)$ until the critical damage (failure) θ_M is attained. Then, for the i^{th} cycle, we have

$$\theta_i = \epsilon\phi_1(\theta_{i-1})\phi_2(p_i) + \theta_{i-1} \tag{7}$$

Defining the damage fraction $\Delta_i = d\theta_i/(\theta_M - \theta_0)$, we obtain the total accumulated damage from Eq. (5) as

$$\xi_i = \sum_{j=1}^{i} \Delta_j = \frac{\sum_{j=1}^{i} d\theta_j}{\theta_M - \theta_0} = \frac{\theta_i}{\theta_M - \theta_0} \tag{8}$$

We can easily verify that $\xi_M = \sum_{j=1}^{M} \Delta_j = 1$. From Eq. (8), we obtain

$$\begin{aligned} d\xi_i &= \frac{d\theta_i}{\theta_M - \theta_0} = \frac{\epsilon}{\theta_M - \theta_0}\phi_1(\theta_{i-1})\phi_2(p_i) \\ &= \frac{\epsilon}{\theta_M - \theta_0}\phi_1((\theta_M - \theta_0)\xi_{i-1})\phi_2(p_i) \end{aligned} \tag{9}$$

Eq. (9) has exactly the same form as the Palmgren-Miner Eq. (6) with $\eta = \epsilon/(\theta_M - \theta_0)$. This can be interpreted as mapping the damage variable θ ($\theta_0 \leq \theta \leq \theta_M$) to degradation measure ξ ($\xi_0 \leq \xi \leq 1$). Thus, a modified prognostic model in terms of damage measure is:

$$\begin{aligned} \dot{\mathbf{x}} &= \mathbf{f}(\mathbf{x}, \lambda(\xi), \mathbf{u}) \\ \xi_i &= \eta\phi_1(\xi_{i-1})\phi_2(p_i) + \xi_{i-1} \\ \mathbf{y} &= \mathbf{C}\mathbf{x} + \mathbf{D}\mathbf{u} + \mathbf{v} \end{aligned} \tag{10}$$

The function $\lambda(\xi)$, which maps the degradation measure to a system parameter, is often assumed to be a polynomial [21]:

$$\lambda(\xi) = \sum_{i=0}^{K} \alpha_i \xi^i \tag{11}$$

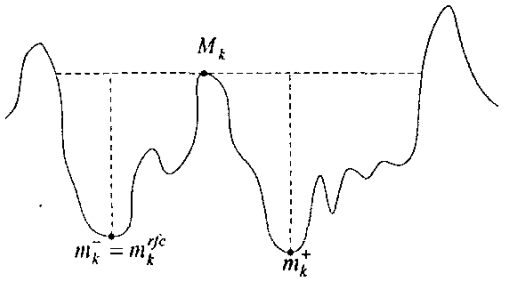

Fig. 4. Definition of the rainflow cycle [23]: From each local maximum M_k, proceed in the left and right directions with as small a downward excursion as possible. The minimum of m_k^- and m_k^+ is defined as rainflow minimum m_k^{rfc}. The k^{th} rainflow cycle is defined as (m_k^{rfc}, M_k)

B. Simulation under random loads (Step 2)

The coupled system model in Eq. (10) is generally nonlinear. Consequently, the evoluation of system dynamics (including fast and slow time) is typically obtained through Monte-Carlo simulations. Since the parameter p is a stochastic process in many applications [20], simulation of Eq. (10) for ξ requires the update of damage parameter ξ for every cycle based on the load parameter p in that cycle. This requires substantially high computation for simulating the system behavior in the slow-time scale.

Here we apply the method of averaging [22] for computational efficiency. In this method, since we are only concerned with the efficient simulation of damage evolution, the averaged equations for the fast variable, $\mathbf{x}$, will not be implemented. For a user specified time T, which corresponds to an intermediate time scale over which the fast time data is collected ($0 < T \ll \eta^{-1}$), define $\mathbf{x}_i(\mathbf{x}_{i-1}, \lambda(\xi_{i-1}))$ as the solution of the unperturbed Eq. (10) with $\eta = 0$, $\xi = \xi_{i-1}$, and initial conditions $\mathbf{x}_{i-1}$. Let the cycle number n_i and load parameter $\{p_i^j\}_{j=1}^{n_i}$ be obtained through some cycle counting method (such as rainflow, mean-crossing, etc. [20]) based on the stress/strain information during the time interval $[0, T]$, which is assumed to be a function of $\mathbf{x}_i$. In this paper, we will adopt the most commonly used cycle counting method, viz., the rainflow method. The definition of rainflow cycle is shown in Fig. 4. This method is able to catch both slow and rapid variations of load by forming cycles that pair high maxima

[1] In some applications, monotonic nonlinear transformation of ξ such as $\ln\xi$ may reduce the variance of remaining life estimates.

with low minima, even if they are separated by intermediate extremes [24]. Defining the function $q(\xi_{i-1}, \{p_i^j\}_{j=1}^{n_i}) = \phi_1(\xi_{i-1})\phi_2(\{p_i^j\}_{j=1}^{n_i})$, we obtain the averaged function:

$$\bar{q} \doteq \frac{1}{n_i}\sum_{j=1}^{n_i} q(\xi_{i-1}, p_i^j) = \frac{\phi_1(\xi_{i-1})}{n_i}\sum_{j=1}^{n_i}\phi_2(p_i^j) \qquad (12)$$

Consequently, we obtain the updated degradation measure as

$$\xi_i - \xi_{i-1} = n_i\bar{q} \Rightarrow \xi_i = \eta\phi_1(\xi_{i-1})\sum_{j=1}^{n_i}\phi_2(p_i^j) + \xi_{i-1} \qquad (13)$$

Note that the update of ξ in Eq. (13) is based on time T, while in Eq. (10) it is based on every cycle. The initial degradation measure ξ_0 is assumed to be a Gaussian random variable $\mathcal{N}(\mu, \sigma^2)$, where μ and σ represent the mean and the standard deviation, respectively.

C. Prognostic modeling (Step 3)

Prognostic modeling is concerned with the dynamics of degradation measure. Consider a system excited under L different random load conditions as being in Modes $1 - L$. Assume that M Monte-Carlo simulations are performed for each random load condition. Then, we can construct L models, one for each mode. The dynamic evolution of degradation measure is given by:

$$\xi_m(k+1) = \beta_m(\xi_m(k)) + v_m(k) \quad k = 0, 1, \ldots \qquad (14)$$

where m is the mode number, β_m is a function of previous state $\xi_m(k)$ and $v_m(k)$ is a zero mean white Gaussian noise with variance $\hat{Q}_m(k)$. The state prediction (function β_m) in IMM for mode m is obtained as follows.

For M Monte-Carlo simulations associated with each mode ($1 \leq m \leq L$), we form the degradation measure:

$$\xi = \psi_m^i(kT) \quad k = 0, 1, \ldots; \; i = 1, 2, \ldots, M \qquad (15)$$

where i is the Monte-Carlo run number under mode m, and T is the sampling interval, which is chosen as an intermediate time scale ($0 < T \ll \eta^{-1}$). Suppose $\hat{\xi}_m(k|k)$ is the state estimate at time k corresponding to mode m, then the residual time is obtained by taking the inverse of Eq. (15):

$$t_m^i(k) = (\psi_m^i)^{-1}[\hat{\xi}_m(k|k)] \qquad (16)$$

Since $\psi_m^i(kT)$ is a discrete-time function, $t_m^i(k)$ in Eq. (16) needs to be obtained through interpolation. The state prediction from the i^{th} Monte-Carlo run of mode m is:

$$\hat{\xi}_m^i(k+1|k) = \psi_m^i(t_m^i(k) + T) \qquad (17)$$

Then, the state prediction and its variance for mode m is:

$$\hat{\xi}_m(k+1|k) = \frac{1}{M}\sum_{i=1}^{M}\hat{\xi}_m^i(k+1|k) \qquad (18)$$

$$\hat{Q}_m(k) = \frac{1}{M-1}\sum_{i=1}^{M}[\hat{\xi}_m^i(k+1|k) - \hat{\xi}_m(k+1|k)]^2$$

Note that the prognostic model discussed above can be computed off-line based on the simulation (or historical) data. Thus, the state prediction equation will be:

$$\hat{\xi}_m(k+1|k) = \beta_m(\hat{\xi}_m(k|k)) \quad k = 0, 1, \ldots \qquad (19)$$

where β_m is a numerically calculated nonlinear function as in Eq. (16-18).

D. Feature parameter estimation (Step 4)

Since the hidden variable ξ is unobserved, we need to estimate it from the input/output data $\{\mathbf{y}, \mathbf{u}\}$. One way to estimate ξ is to use the update equation for ξ in Eq. (10), where $\phi_2(p_i)$ is a function of measurement $\mathbf{y}$. Since we do not know the initial value of ξ_0, this method will produce biased estimates.

Another method is based on estimation of the drifting parameter λ of the fast time process in Eq. (10). Two parameter estimation techniques, equation error method and output error method, can be employed to estimate λ from a time history of measurements $\{\mathbf{u}(t), \mathbf{y}(t)\}_{t=0}^{T}$ [2]. During the time interval $[t, \; t + \alpha T]$, we assume that the parameter λ is a constant (typically $\alpha \simeq 1/10$). Generally, equation error method is computationally more efficient than the output error method. However, it is less accurate than the output error method. The accuracy of equation error method can be improved by increasing the number of data points for parameter estimation. Details of parameter estimation can be found in [2], [25]. Here, we employ the equation error method to estimate λ.

In the equation-error method, the governing equation for estimating λ is the residual equation. The residual equation $r(\mathbf{y}, \mathbf{u}, \lambda)$ is the rearranged form of the input-output or state-space model of the system. Suppose N data points of the fast-time process are acquired in an intermediate time interval $[t, \; t + \alpha T]$. Then, the optimal parameter estimate is given by:

$$\lambda^* = \underset{\lambda^*}{argmin}\sum_{i=1}^{N}\|r(y_i, u_i, \lambda)\|^2 \qquad (20)$$

Based on the internal structure of the residual equation, two optimization algorithms, linear least squares and nonlinear least squares, can be implemented. If prior knowledge on the range of λ is available, the problem can be solved via constrained optimization. In any case, we can construct the measurement equation as:

$$z(k) = \lambda(\xi(k)) + \kappa(k) \quad k = 0, 1, 2, \ldots \qquad (21)$$

where $z(k) = \lambda^*$, $\lambda(\xi)$ is typically a polynomial function as in Eq. (11) and$\kappa(k)$ is a zero mean Gaussian noise with variance $\hat{S}(k)$. The variance is obtained as a by-product of the parameter estimation method.

E. Track the degradation measure (Step 5)

To track the degradation measure, an interacting multiple model (IMM) estimator [13], [26] is implemented for online estimation of the damage variable. For a system with L operational modes, there will be L models in IMM, one for

each mode. Each model will have its own dynamic equation as in Eq. (14) and the measurement equation as in Eq. (21). Details of IMM filter can be found in [13].

F. Predict the remaining life (Step 6)

The remaining life depends on the current damage state $\xi(k)$, as well as the future usage of the system. If the future operation of a system is known a priori, the remaining life can be estimated using the knowledge of future usage. Typically, one considers three type of prior knowledge.

1) Deterministic operational sequence: In this case, we assume that the system will be operated according to a known sequence of mode changes and mode durations. Define a sequence $S = \{m_i, T_{si}, T_{ei}\}_{i=1}^{Q}$, where T_{si} and T_{ei} represent the start time and the end time under mode m_i, such that $T_{s1} = 0$, $T_{ei} = T_{si+1}$, and T_{sQ} is the time at which $\xi = 1$. Suppose M Monte-Carlo simulations are performed for this operational sequence. Then we obtain M remaining life estimates based on $\hat{\xi}(k|k)$, the damage estimate at time instant k. The mean remaining life estimate and its variance are obtained from these M estimates via relations similar to Eq. (18).

2) Probabilistic operational sequences: In this case, we assume that the system is operated under J operational sequences $S_j = \{m_i^j, T_{si}^j, T_{ei}^j\}_{j=1}^{J}$, where S_j is assumed to occur with a known probability ζ_j. If $\hat{r}_j(k)$ is the estimate of residual life based on sequence S_j, then the remaining life estimate $\hat{r}(k)$, and its variance $P(k)$, are given by:

$$\hat{r}(k) = \sum_{j=1}^{L} \zeta_j(k)\hat{r}_j(k)$$
$$P(k) = \sum_{j=1}^{L} \zeta_j(k)\{P_j(k) + [\hat{r}_j(k) - \hat{r}(k)]^2\} \qquad (22)$$

3) On-line sequence estimation: This method estimates the operational sequence based on measured data via IMM mode probabilities. Here, we assume that future operation of this system will follow the observed history and the dynamics of mode changes. Suppose we obtain the residual time $t_m^i(k)$ according to Eq. (16) for the i^{th} Monte-Carlo run in mode m. Then, we can calculate the time to failure for $\xi = 1$ as:

$$t_m^i(end) = (\psi_m^i)^{-1}[1] \qquad (23)$$

The remaining life estimate from i^{th} Monte-Carlo run for mode m is:

$$\hat{r}_m^i(k) = t_m^i(end) - t_m^i(k) \qquad (24)$$

Then, the remaining life estimate and its variance for mode m is:

$$\hat{r}_m(k) = \frac{1}{M}\sum_{i=1}^{M} \hat{r}_m^i(k) \qquad (25)$$
$$P_m(k) = \frac{1}{M-1}\sum_{i=1}^{M} [\hat{r}_m(k) - \hat{r}_m^i(k)]^2$$

The above calculation can be performed off-line based on simulated (or historical) data. To reflect the operational history, we use the mode probabilities from IMM to estimate the remaining life as follows.

Let $\mu_j(k)$, $\bar{\mu}_j(k)$ denotes the mode probability and averaged mode probability for mode $j = 1, 2, ..., L$ under damage measure $\hat{\xi}(k|k)$. The averaged mode probability is initialized as $\bar{\mu}_j(0) = 1/L$. The recursive updates for the averaged mode probability, the remaining life estimate and its variance for $k \geq 1$ are:

$$\bar{\mu}_j(k) = \frac{1}{k}[(k-1)\bar{\mu}_j(k-1) + \mu_j(k)] \quad for\ j = 1, 2, ..., L;$$
$$\hat{r}(k) = \sum_{j=1}^{L} \bar{\mu}_j(k)\hat{r}_j(k)$$
$$P(k) = \sum_{j=1}^{L} \bar{\mu}_j(k)\{P_j(k) + [\hat{r}_j(k) - \hat{r}(k)]^2\} \qquad (26)$$

Note that the remaining life prediction $\hat{r}(k)$ and $P(k)$ will decrease as degradation measure ξ increases. This implies that as the damage measure ξ approaches 1, we can obtain more accurate estimates of the remaining life (i.e., less uncertainty).

V. Demonstration of the Prognostic Process

To demonstrate the prognostic algorithms, a simulation study is conducted on an automotive suspension system. A half-car two degree of freedom model [27] is adopted. The active suspension part is not used in our simulation. Fig. 5 shows the suspension model, which is subject to irregular excitation from a road surface. This demonstration will follow the prognostic process discussed in the previous section.

The equations of the model are given by

$$\begin{aligned}
&m\ddot{x} + (f_{ca} + f_{ka}) + (f_{cb} + f_{kb}) = 0 \qquad (27)\\
&I\ddot{\theta} + l_a(f_{ca} + f_{ka}) - l_b(f_{cb} + f_{kb}) = 0\\
&m_{2a}\ddot{x}_{2a} - (f_{ca} + f_{ka}) + k_{2a}(x_{2a} - w_a) = 0\\
&m_{2b}\ddot{x}_{2b} - (f_{cb} + f_{kb}) + k_{2b}(x_{2b} - w_b) = 0\\
&x = (l_b x_{1a} + l_a x_{1b})/l,\ \theta = (x_{1a} - x_{1b})/l\\
&l = l_a + l_b\\
&f_{ci} = c_i(\dot{x}_{1i} - \dot{x}_{2i}),\ i = a, b\\
&f_{ki} = k_{1i}(x_{1i} - x_{2i}),\ i = a, b
\end{aligned}$$

where

m : vehicle mass — I : moment of inertia
m_{2a} : mass of front wheel — m_{2b} : mass of rear wheel
θ : rotary angle of vehicle — x : vertical displacement
f_{ca}, f_{cb} : damping force of the front/rear wheel
f_{ka}, f_{kb} : restoring force of the front/rear wheel
k_{1a}, k_{1b} : spring constants of the front/rear suspension
k_{2a}, k_{2b} : spring constants of the front/rear suspension
x_{2a}, x_{2b} : vertical displacement of the front/rear wheel
x_{1a}, x_{1b} : displacement of the vehicle body at front/rear
l_a, l_b : distance of the front/rear suspension to center
w_a, w_b : irregular excitations from the road surface

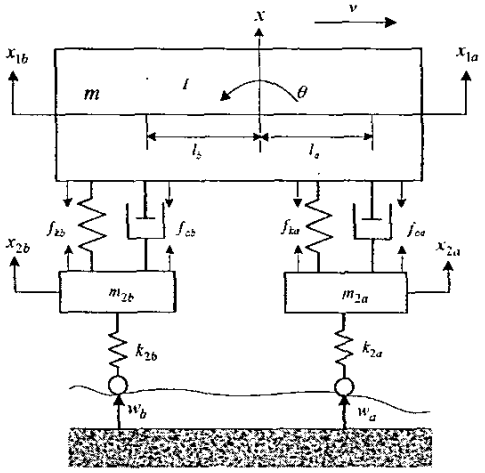

Fig. 5. Half-car suspension model

A. Identify system model

The model parameters are obtained from [27], [28]:

$$\begin{aligned} &m_{2a} = 30\ (kg) && I = 2100\ (kgm^2) \\ &m_{2b} = 25\ (kg) && m = 1200\ (kg) \\ &k_{2a} = k_{2b} = 152\ (kN/m) \\ &l_a = 0.9\ (m) && l_b = 1.2\ (m) \\ &c_b = 4000\ (N/m/s) && c_a = 5000\ (N/m/s) \\ &k_{1a} = 56000\ (N/m) && k_{1b} = 42000\ (N/m) \end{aligned}$$

The standard vector matrix form of Eq. (27) is:

$$\mathbf{M}\ddot{\mathbf{z}} + \mathbf{N}\dot{\mathbf{z}} + \mathbf{K}\mathbf{z} = \mathbf{E}\mathbf{u} \tag{28}$$

where the state, input (excitation vectors) are given by

$$\mathbf{z} = (x_{1a}\ x_{2a}\ x_{1b}\ x_{2b})^T \qquad \mathbf{u} = (w_a\ w_b)^T$$

It is assumed that the vertical accelerations $\ddot{x}_{1a}, \ddot{x}_{1b}, \ddot{x}_{2a}, \ddot{x}_{2b}$ are the measured variables. The $\mathbf{M}, \mathbf{N}, \mathbf{K}$ and $\mathbf{E}$ matrices are given by:

$$\mathbf{M} = \begin{bmatrix} l_b m/l & 0 & l_a m/l & 0 \\ I/l & 0 & -I/l & 0 \\ 0 & m_{2a} & 0 & 0 \\ 0 & 0 & 0 & m_{2b} \end{bmatrix}$$

$$\mathbf{N} = \begin{bmatrix} c_a & -c_a & c_b & -c_b \\ l_a c_a & -l_a c_a & -l_b c_b & l_b c_b \\ -c_a & c_a & 0 & 0 \\ 0 & 0 & -c_b & c_b \end{bmatrix}$$

$$\mathbf{K} = \begin{bmatrix} k_{1a} & -k_{1a} & k_{1b} & -k_{1b} \\ l_a k_{1a} & -l_a k_{1a} & -l_b k_{1b} & l_b k_{1b} \\ -k_{1a} & k_{1a}+k_{2a} & 0 & 0 \\ 0 & 0 & -k_{1b} & k_{1b}+k_{2b} \end{bmatrix}$$

$$\mathbf{E} = \begin{bmatrix} 0 & 0 \\ 0 & 0 \\ k_{2a} & 0 \\ 0 & k_{2b} \end{bmatrix}$$

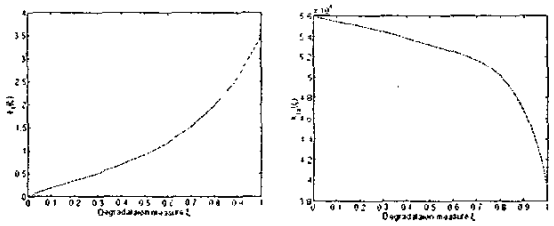

Fig. 6. Function $\phi_1(\xi)$, $k_{1a}(\xi)$ versus the degradation measure ξ

The second order linear dynamic model (27) can be represented in state space by introducing the state vector

$$\mathbf{x} = \begin{bmatrix} \mathbf{z}(t) \\ \dot{\mathbf{z}}(t) \end{bmatrix}, \qquad \dot{\mathbf{x}} = \begin{bmatrix} \dot{\mathbf{z}}(t) \\ \ddot{\mathbf{z}}(t) \end{bmatrix}$$

Eq. (27) is transformed to the equivalent state space form:

$$\begin{aligned} \dot{\mathbf{x}} &= \mathbf{A}\mathbf{x} + \mathbf{B}\mathbf{u} \\ \mathbf{y} &= \mathbf{C}\mathbf{x} + \mathbf{D}\mathbf{u} + \mathbf{v} \end{aligned} \tag{29}$$

where

$$\mathbf{A} = \begin{bmatrix} \mathbf{0} & \mathbf{I}_n \\ -\mathbf{M}^{-1}\mathbf{K} & -\mathbf{M}^{-1}\mathbf{N} \end{bmatrix}$$

$$\mathbf{B} = \begin{bmatrix} \mathbf{0} \\ \mathbf{M}^{-1}\mathbf{E} \end{bmatrix}$$

$$\mathbf{C} = \mathbf{M}^{-1}\begin{bmatrix} -\mathbf{K} & -\mathbf{N} \end{bmatrix}, \quad \mathbf{D} = \mathbf{E}$$

The input $\mathbf{u}$, which is the irregular excitation from the road surface, is generated as follows [29]. The road roughness is typically specified as a random process of a given displacement power spectral density (p.s.d.). An often used approximation of road displacement p.s.d. for various roads is given by

$$S(\omega) = A\omega^q \tag{30}$$

where A and q are appropriate constants. The most commonly used case corresponds to $q = -2$. With this value, the displacement spectra in Eq. (30) implies that the displacement is a Wiener-process. Here, we modify Eq. (30) to make displacement a stationary process. The modified p.s.d. for displacement is $S(\omega) = A/(c^2+\omega^2)$, where c is a small number (here we choose $c = 0.01\ rad/s$). Thus, the displacement input $\mathbf{u} = (w_a\ w_b)^T$ is generated by

$$\dot{w}_i + cw_i = \rho_i, \quad i = a, b \tag{31}$$

where ρ_i is a zero-mean Gaussian random process with the correlation functions:

$$\begin{aligned} E[\rho_i(t)\rho_j(\tau)] &= A\delta(t-\tau) \quad \text{for } i = j \\ &= A\delta(|t-\tau| - t_l) \quad \text{for } i \neq j \end{aligned} \tag{32}$$

where A is the variance of white noise, and $t_l = (l_a + l_b)/v$ is the time delay between the front and rear wheels [27]. We assume that the speed is a constant with a value of $20(m/s)$. According to [29], three road terrains are selected: very good, fair, severe. These terrains are characterized by parameter A.

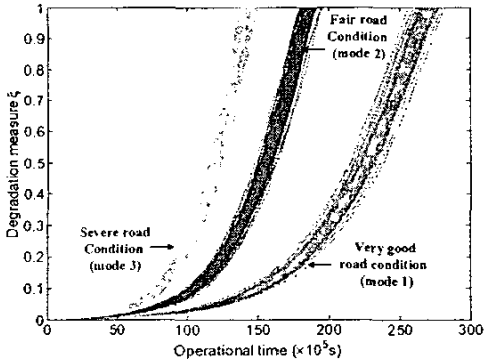

Fig. 7. 100 Monte-Carlo simulations for three random loads

The parameter A for these three roads are $10^{-6}m^2$,$4\times10^{-6}m^2$ and $9 \times 10^{-6}m^2$, respectively. The measurement noise covariance for accelerometer measurements $\mathbf{v} = (v_1\ v_2\ v_3\ v_4)^T$ are assumed to be identical with $\mathcal{N}(0, 10^{-4}\mathbf{I})$. The simulation sampling rate is 2kHz.

Eq. (29) consists of fast-time dynamic equation and measurement equation. To construct a complete model in Eq. (10), we need a slow-time model for the degradation measure ξ. In this model, we assume that the stiffness k_{1a} of front suspension is the coupled parameter that is a function of ξ. The related stiffness degradation function $k_{1a}(\xi)$ is approximated by the following polynomial

$$k_{1a} = \lambda(\xi) = 5.6 \times 10^4 - 8.84 \times 10^3\xi + 4.34 \times 10^4\xi^2 - 1.66 \times 10^5\xi^3 + 2.53 \times 10^5\xi^4 - 1.38 \times 10^5\xi^5 \quad (33)$$

Let us consider the front suspension system with an edge crack that is orthogonal to external loading. In Eq. (3), we assume that $\gamma = 2$. Then, $\phi_1(\theta)$ has the following form [30]:

$$\phi_1(\theta) = (\pi\theta) \times [1.122 - 1.4(\theta/b) + 7.33(\theta/b)^2 - 13.08(\theta/b)^3 + 14(\theta/b)^4]^2 \quad (34)$$

where θ is the crack length and b is the width of the mechanical component of front suspension system. We assume that the maximum θ_M is $b/8$. Defining degradation measure as $\xi = \theta/\theta_M = 8\theta/b$, we obtain the function $\phi_1(\xi)$ needed in Eq. (10) by substituting $\theta = b\xi/8$ in Eq. (34).

Fig. 6 shows these two functions versus the degradation measure ξ. For $\gamma = 2$, the function $\phi_2(p)$ is equal to p^2. The parameter η in Eq. (10) is $\eta = 8\times10^{-6}$. The intermediate time scale T is equal to 100s. The initial damage ξ_0 is assumed to be $\mathcal{N}(10^{-3}, 10^{-4})$.

B. Simulation results

The system model in Eq. (10) was simulated with a standard 4^{th}-order variable-step-size Runge-Kutta algorithm. Fig. 7 shows the results of 100 Monte-Carlo simulations for the system under three different road conditions. Compared to the severe road condition, the increases in the life times for the fair and very good roads are about 35% and 80%, respectively. If

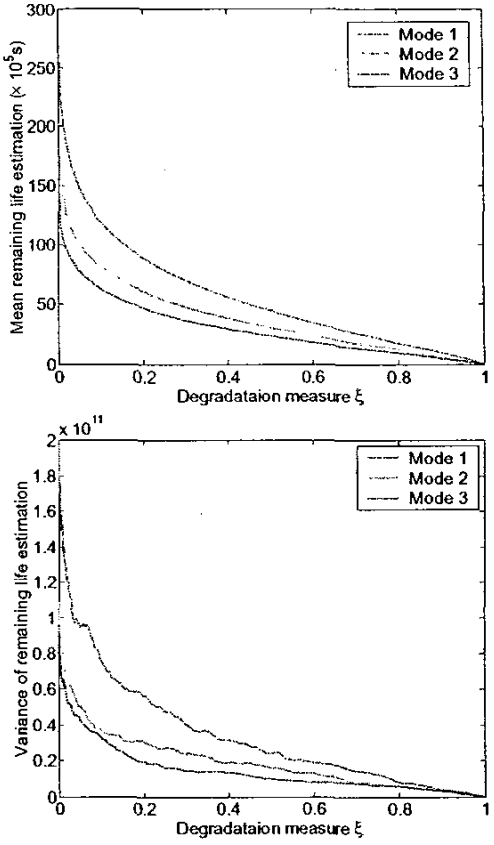

Fig. 8. Mean and variance of remaining life estimate versus degradation measure

we assume a 10% calendar time usage of the automobile (2.4 hours a day), the expected life of suspension system will be 4.5, 6 and 8 years, respectively, for the three road conditions (severe, fair and very good).

C. Prognostic modeling from simulation data

Since the suspension system has three random road conditions, the number of modes in the degradation model of Eq. (14) is 3. The model parameters for each mode are estimated as discussed in the previous section.

D. Feature estimation

In this paper, we use the equation error method to estimate k_{1a}. The residual equation is obtained by substituting the last equation for f_{ka} in the first equation in Eq. (27), and changing state $\mathbf{x}$ to measurement $\mathbf{y}$:

$$r(\mathbf{y}, k_{1a}) = (ml_by_1 + ml_ay_2)/l + c_a(\int y_1 - \int y_2) + c_b(\int y_3 - \int y_4) + k_{1b}(\iint y_3 - \iint y_4) + k_{1a}(\iint y_1 - \iint y_2) \quad (35)$$

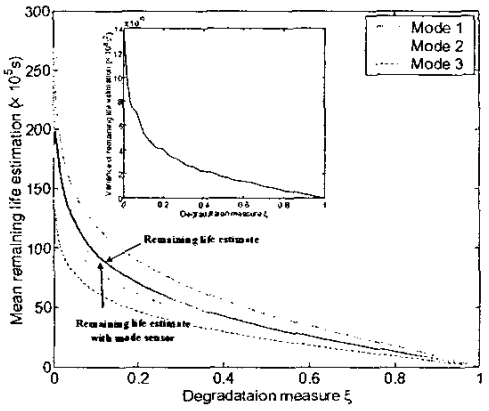

Fig. 9. Estimate of remaining life for single run

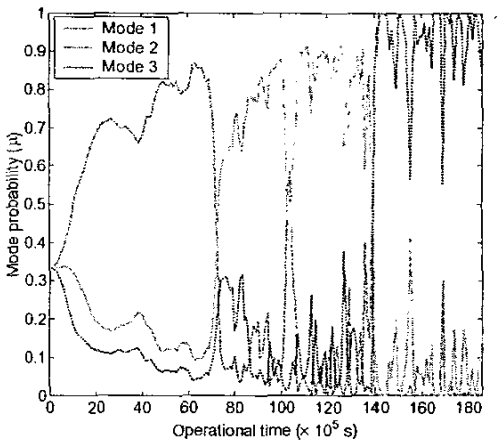

Fig. 10. Mode probabilities of the IMM

where y_1 through y_4 are the measurements. Since the above equation can be written as a standard linear regression model, the value of k_{1a} can be identified through linear least-squares estimation by minimizing $\sum_{i=1}^{N} \|r(y_i, k_{1a})\|^2$, where $N = 0.1T \cdot 2000 = 20,000$ and $T = 100s$. The estimated variance $\hat{S}(k)$ for parameter k_{1a} can also be calculated. The $\hat{S}(k)$ of the parameter estimation is almost the same for a range of k_{1a} values we simulated for each mode. We use $\hat{S}(k) = 2.6 \times 10^4\ N^2/m^2$.

E. Track the degradation measure

For IMM implementation, we use the following transition matrix:

$$\Phi = \begin{bmatrix} 0.9 & 0.05 & 0.05 \\ 0.05 & 0.9 & 0.05 \\ 0.05 & 0.05 & 0.9 \end{bmatrix}$$

where $\Phi_{ij} = P(\text{mode } j \text{ in effect at time } k+1 \mid \text{mode } i \text{ in effect at time } k)$. The system mode changes are simulated as follows. Mode 1:$[0, 70\times10^5 s]$, Mode 2:$[70, 140\times10^5 s]$, Mode 3:$[140 \times 10^5 s, t_{end}]$, where t_{end} is the time at which $\xi = 1$.

Fig. 10 shows the plot of mode probabilities of the IMM. The mode probabilities for the three modes are initialized to $(\bar{\mu}_j(0) = 1/3,\ j = 1,2,3)$ and then Mode 1 reaches the highest mode probability (approximately 0.85) in the range $[0, 70 \times 10^5 s]$. Mode 2 reaches the highest mode probability (approximately 0.9) in the range $[70 - 140 \times 10^5 s]$. Finally Mode 3 dominates the remainder of simulation with the highest probability around 0.99. Thus, the IMM (which may be viewed as a software sensor) tracks the road condition very well based on noisy data.

F. Predict remaining life

The mean remaining life estimate $\hat{r}_j(k)$ and its variance $P_j(k)$ under the three modes are calculated off-line according to Eq. (23-25). Fig. 8 presents the mean and variance of remaining life estimate for the three modes. The nonlinear relationship between the degradation measure ξ and the mean remaining life estimates is clearly evident. These values and mode probabilities from IMM are used in Eq. (26) to recursively obtain the remaining life estimate of the suspension system. Fig. 9 presents the estimate of remaining life (solid bold line) and its variance using IMM mode probabilities in Eq. (18) for a single run of the scenario considered in subsection *E*. We can see that, initially, the remaining life estimate follows Mode 1 and after switching to Mode 2, the remaining life estimate is in between those of Modes 1 and 2, which is what one would expect. Finally, the remaining life estimate approaches that corresponding to Mode 2. The dashed bold line represents the remaining life estimates assuming that the road surface condition can be measured accurately via a sensor (such as an infrared sensor). In this case, the mode is known. We can evaluate the contribution of the additional sensor to the accuracy of the remaining life estimate. In Fig. (9), we can see the IMM produces remaining life estimates that are close to the estimates that one would get with the additional displacement sensor. The difference between these two estimates is relatively high (about 6%) at the beginning ($\xi < 0.1$) and they are virtually identical as degradation measure ξ increases.

Fig. 11 shows the root mean square error (RMSE) of the estimates of remaining life. At the beginning ($\xi < 0.02$), RMS errors are high due to the transient effects of the IMM filter. After that, the RMS error rapidly becomes small as degradation measure increases. The RMS is in the order of 10^2 to 10^1 hours of usage (40 to 4 days of calendar time), which is very accurate compared to the total life of the suspension system.

VI. Conclusion

Unlike conventional maintenance strategies, prognostic techniques predict system degradation based on observed system condition to support "just-in-time" maintenance. The ever increasing usage of model-based design technology facilitates the integration of model-based diagnosis and prognosis of systems, leading to condition-based maintenance.

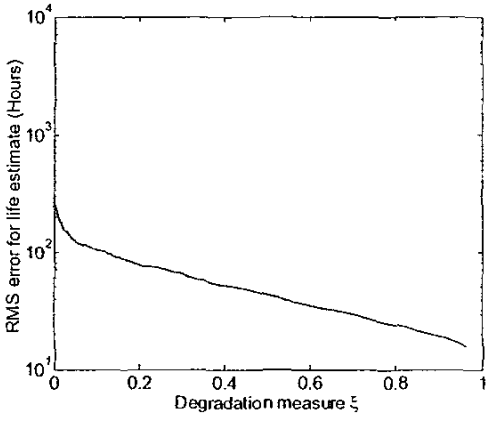

Fig. 11. RMS remaining life time estimate error

In this paper, a systematic model-based prognostic process was presented to predict the remaining life of a system with multiple operational modes. We uses singular perturbation methods of control theory, coupled with dynamic state estimation techniques. An IMM filter was implemented to estimate the degradation measure. The time-averaged mode probabilities are used to predict the remaining life. This process was demonstrated on an automotive suspension system with a drifting parameter.

There are several future extensions of this research work. These include the refinement of the prognostic process, application of the process to real-world systems, and incorporation of stochastic models of degradation.

ACKNOWLEDGMENT

The support for this research by the Toyota Technical Center is gratefully acknowledged. Any opinions expressed in this paper are solely those of the authors and do not represent those of the sponsor.

REFERENCES

[1] B. Terry and S. Lee, "What is the prognosis on your maintenance program," *Engineering and Mining Journal*, May 1995.

[2] J. Luo, F. Tu, M. Azam, K. Pattipati, L. Qiao, and M. Kawamoto, "Intelligent model-based diagnostics for vehicle health management," in *SPIE Conference Proceedings*, Orlando, April 2003.

[3] S. Deb, K. R. Pattipati, V. Raghavan, M. Shakeri, and R. Shrestha, "Multi-signal flow graphs: a novel approach for system testability analysis and fault diagnosis," *Aerospace and Electronic Systems Magazine*, vol. 10, no. 5, pp. 14 –25, 1995.

[4] F. Barbera, H. Schneider, and P. Kelle, "A condition based maintenance model with exponential failures and fixed inspection intervals," *Journal of Operational Research Society*, vol. 47, pp. 1037–1045, 1996.

[5] J. J. Tom Brotherton, Gary Jahns and D. Wroblewski, "Prognosis of faults in gas turbine engines," in *Proc. IEEE International Conference on Aerospace*, vol. 6, 2000, pp. 163 –171.

[6] L. H. Chiang, E. Russel, and R. Braatz, *Fault detection and diagnosis in industrial systems*. London: Springer-Verlag, 2001.

[7] W. Yang, "Towards dynamic model-based prognostics for transmission gears," in *SPIE Conference Proceedings*, vol. 4733, 2001, pp. 157–167.

[8] W. Wang and A. Wong, "Autoregressive model based gear fault diagnosis," *Journal of Vibration and Acoustics*, vol. 124, pp. 172–179, 2002.

[9] Q. Zhang, M. Basseville, and A. Benveniste, "Early warning of slight changes in systems," *Automatica*, vol. 30, pp. 95–114, 1994.

[10] P. Wang and G. Vachtsevanos, "Fault prognosis using dynamic wavelet neural networks," in *Maintenance and Reliability Conference. MARCON 99*, May 1999.

[11] D. Swanson, "A general prognostic tracking algorithm for predictive maintenance," in *Proc. IEEE International Conference on Aerospace*, vol. 6, 2001, pp. 2971–2977.

[12] A. K. Garga, K. T. Mcclintic, R. L. Campbell, C.-C. Yang, and M. S. Lebold, "Hybrid reasoning for prognostic learning in cbm systems," in *IEEE*, 2000, pp. 2957–2969.

[13] Y. Bar-Shalom, X.-R. Li, and T. Kirubarajan, *Estimation with applications to tracking and navigation*. John Wiley and Sons, INC., 2001.

[14] D. E. Adams, "Nonlinear damage models for diagnosis and prognosis in structural dynamic systems," in *SPIE Conference Proceedings*, vol. 4733, 2002, pp. 180–191.

[15] D. Chelidze, "Multimode damage tracking and failure prognosis in eletromechanical system," in *SPIE Conference Proceedings*, vol. 4733, 2002, pp. 1–12.

[16] D. Chelidze, J.P.Cusumano, and A. Chatterjee, "Dynamical systems approach to damage evolution tracking, part I: The experimental method," *Journal of Vibration and Acoustics*, vol. 124, pp. 250–257, 2002.

[17] P. V. Kokotovic, H. K. Khail, and J. O'Reilly, *Signular perurbation methods in control: analysis and design*. Orlando, Florida: Academic Press INC., 1986.

[18] N. Berglund and B. Gentz, "Geometric singular perturbation theory for stochastic differential equations," *Journal of Differential Equations*, vol. 191, pp. 1–54, 2003.

[19] M. Todinov, "Necessary and sufficient condition for additivity in the sense of palmgren-miner rule," *Computational Materials Science*, vol. 21, pp. 101–110, 2001.

[20] K. Sobczyk and B. Spencer, *Random fatigue: from data to theory*. San Diego: Academic Press INC., 1993.

[21] K. Sobczyk and J. Trebicki, "Stochastic dynamics with fatigue-induced stiffness degradation," *Probabilistic Engineering Mechanics*, vol. 15, no. 1, pp. 91–99, 2000.

[22] J. Sanders and F. Verhulst, *Averaging methods in nonlinear dynamic systems*. New York: Springer-Verlag, 1985.

[23] I. Rychlik, "A new definition of the rainflow cycle counting method," *Internationaly Journal of Fatigue*, vol. 9, pp. 119–121, 1987.

[24] Johannesson, "Rainflow cycles for switching processes with markov structure," *Probability in the Engineering and Informational Sciences*, vol. 12, no. 2, pp. 143–175, 1998.

[25] L. Ljung, *System identification: theory for the user*. New Jersey: Prentice-Hall INC., 1987.

[26] E. Phelps and P. Willett, "Useful lifetime tracking via the imm," in *SPIE Conference Proceedings*, vol. 4733, 2002, pp. 145–156.

[27] T. Yoshimura, K. Nakaminami, M. Kurimoto, and J. Hino, "Active suspension of passenger cars using linear and fuzzy-logic controls," *Control Engineering Practice*, vol. 41, pp. 41–47, 1999.

[28] *Using Simulink and Stateflow in Automotive Applications*. The MathWorks, Inc., 1998.

[29] D. Hrovat, "Survey of advanced suspension developments and related optimal control applications," *Automatica*, vol. 33, no. 10, pp. 1781–1817, 1997.

[30] J. Lemaitre and J. Chaboche, *Mechanics of solid materials*. NewYork: Cambridge University Press, 1990.